Available online at www.sciencedirect.com
ScienceDirect
Acta Materialia 58 (2010) 5097–5108
Acta MATERIALIA
www.elsevier.com/locate/actamat

Influence of interface energies on solute partitioning mechanisms in doped aluminas

Shen J. Dillon [a,*], Martin P. Harmer [b], Gregory S. Rohrer [c]

[a] University of Illinois, Materials Science and Engineering, 1304 West Green Street, Champaign, IL 61801, USA
[b] Lehigh University, Center for Advanced Materials and Nanotechnology, 5 East Packer Avenue, Bethlehem, PA 18015, USA
[c] Carnegie Mellon University, Department of Materials Science and Engineering, 5000 Forbes Avenue, Pittsburgh, PA 15213, USA

Received 8 February 2010; received in revised form 20 May 2010; accepted 23 May 2010
Available online 18 June 2010

Abstract

The experiments described in this paper have been designed to understand how particular dopants in alumina (Ca, Mg, Si, and Y) affect microstructural development through the energetics of their associated precipitates. Specifically, the role of the interphase boundary energy and precipitation activation energy are considered to be in competition with grain boundary complexion (disorder) transitions for partitioning excess solute. The results reveal a relationship between the relative precipitation activation energy and the temperature at which grain boundary complexion transitions occur. The large differences in activation energy primarily derive from the interphase boundary energy. Precipitates that form lower interphase boundary energies tend to suppress complexion transitions, while systems that contain precipitates with high interphase boundary energies are more susceptible. Based on the findings, a new criterion for additive selection to control complexion transitions and abnormal grain growth is proposed that is based on interfacial energies between the host and precipitate.

Keywords: Grain growth; Interfaces; Grain boundary; Abnormal grain growth; Sintering

1. Introduction

The microstructural evolution of polycrystalline materials is known to be influenced by chemical additives. Dopants and additives in relatively low concentrations may impact on a material's microstructural evolution and resultant properties. While scientific guiding principles to make informed decisions about additive chemical selection would be useful, they are typically selected by trial and error or empiricism. A classic example of this is the use of magnesia to prevent abnormal grain growth in alumina [1]. A few hundred parts per million of magnesia can reduce the grain boundary mobility of alumina by several orders of magnitude [2–4]. Typical theories for the role of magnesia as a sintering aid in alumina have related to solute drag, particle drag, defect chemistry, and interfacial energy effects [2,5–15]. While each of these effects appears to be important, other dopants selected based on these criteria alone have not produced expected trends [2]. Therefore, many of the existing models for abnormal grain growth are still questionable. Similarly, a recent, thorough, study of abnormal grain growth in copper-doped aluminum revealed that none of the classic models could sufficiently explain the results in this metallic system [16]. Developing better additive selection criteria will enable informed microstructural and materials design, which ultimately impacts performance and properties.

A new concept for understanding grain boundary chemistry, structure, and segregation has been proposed recently [17–19]. It suggests that an analogy exists between grain boundaries and phases in that they are transformable as a function of relevant thermodynamic properties. The difference is that grain boundary "phases" or complexions are thermodynamically stable only in the presence of the abutting crystals. Complexions have typically been

* Corresponding author. Tel./fax: +1 217 333 5622.
E-mail address: sdillon@illinois.edu (S.J. Dillon).

1359-6454/$36.00 © 2010 Acta Materialia Inc. Published by Elsevier Ltd. All rights reserved.
doi:10.1016/j.actamat.2010.05.045

observed as disordered or structurally transformed grain boundaries that often have characteristic features, such as "equilibrium" thickness. The concept has been discussed in several recent review articles [20–24]. Alumina grain boundaries may display several different complexions depending on chemistry and temperature. Different complexions may have vastly different kinetics. Abnormal grain growth will result from the coexistence of two different complexions. An additive that stabilizes a single complexion will promote normal grain growth, and an additive that stabilizes multiple complexions with different mobilities at a single temperature will cause abnormal grain growth. Results of experiment and theory suggest that multiple complexions may coexist at a single temperature because their stability is a function of grain boundary character, because the occurrence of transitions may be subject to Boltzmann statistics, and because they may exist metastably [17].

Magnesia has been shown to favor the stabilization of ordered complexions in alumina that have lower mobilities [17]. Other dopants, such as silica and calcia, have been shown to promote the formation of a range of more disordered complexions that result in enhanced kinetics and abnormal grain growth [17,25,26]. Abnormal grain growth resulting from the formation of disordered complexions has been shown to occur in yttria-doped alumina, but it is still unclear how much of the effect relates to the yttria or the presence of other trace impurities [27–29]. Understanding why these dopants behave so differently has been an ongoing challenge. For example, magnesia and calcia are both divalent cations, both segregate strongly to the grain boundary, and both form precipitates that may cause drag. However, calcia doping promotes abnormal grain growth, while magnesia suppresses it.

Anisotropy has been known to play a role in microstructural evolution, as shown in Fig. 1a and b. For example, calcia doping is well known to produce large plate-like abnormal grains in alumina [30–34]. This morphology results from the coexistence of two different complexions on different planes of the abnormal grain [17]. Specifically, under certain conditions, complexion transitions are less likely to occur on the basal planes than other competing planes [25]. Understanding these complex differences will provide insight into future materials design and property improvement. For example, these types of plate-like grains have been used to produce toughened microstructures [35].

Recent work has shown that the first complexion transition to occur in alumina as the material is heated produces a decrease in the average energy of the abnormal grain boundaries relative to the normal grain boundaries in the same sample (~20–40% reduction) [36]. In this case, the results indicate that a significant portion of the normal grain boundary population is metastable relative to the abnormal population [36]. These results suggest that the activation energy associated with disordering the grain boundary during this first transition is often large and is likely to affect the probability for the occurrence of a complexion transition. If the transitions are activation limited they should follow Boltzmann statistics, where the fraction that has undergone a transition relates to the ratio of the activation energy (ΔE) to kT. The population of boundaries that has undergone a complexion transition is often low in the temperature range of interest to the phenomenon of abnormal grain growth, suggesting that $\Delta E/kT$ is often less than unity in this range for alumina. Grain boundaries are apparently supersaturated by solute at the onset of both precipitation and abnormal grain growth [29,37]. Supersaturation is also indicative of an activation barrier to a chemically induced phase change. This is important because other processes may compete with the complexion transition, and the most energetically favorable process will dominate. Thermodynamic theory predicts that complexion transitions may occur in single-phase regions [17–19]. This simply means that the change in free energy (ΔG) associated with a complexion transition may be negative in single-phase regions. However, the authors are unaware

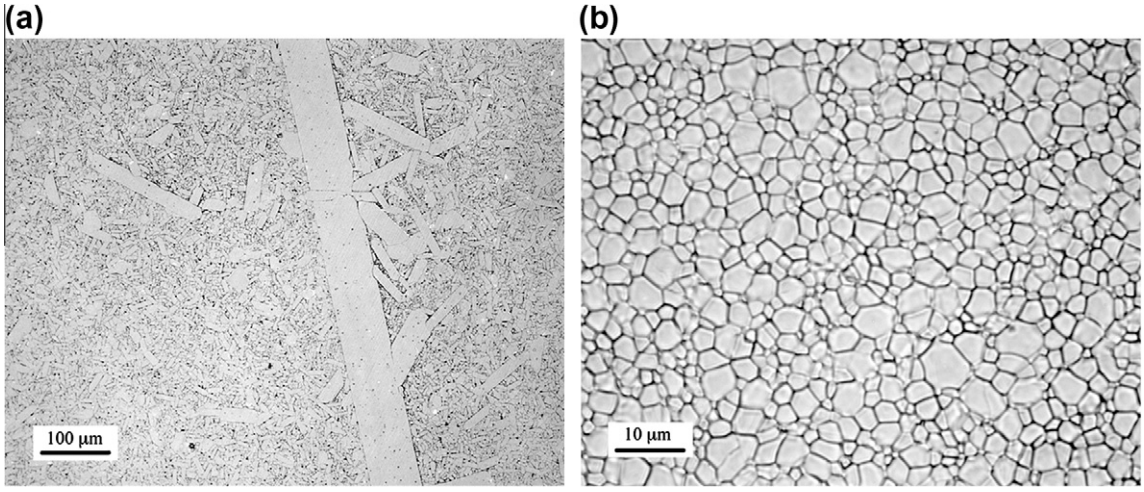

Fig. 1. Optical micrographs of (a) calcia-doped alumina annealed at 1750 °C and (b) magnesia-doped alumina annealed at 1700 °C.

of any observations of complexions, such as the widely observed intergranualr film, in systems processed in a single-phase region. This fact may suggest that although $\Delta G < 0$ for complexion transitions may occur in a single-phase region, it may not be possible to overcome the activation barrier associated with that transition without supersaturation. The prior work by the authors always observed a small amount of precipitates by transmission electron microscopy or transmission optical microscopy and dopant concentrations were chosen to be slightly above reported solubility limits [17]. Therefore, it is worth noting that complexion transitions and precipitation reactions may occur in the same system and that they might compete energetically at different boundaries to affect their relative distribution.

When solute is present at levels above the lattice solubility of a single crystal, the grain boundaries will be enriched. As grain growth proceeds and grain boundary area decreases, the concentration of excess solute in the grain boundary increases to the grain boundary saturation limit. As growth continues and the concentration increases above the grain boundary solubility limit, the excess solute must be accommodated elsewhere. There are several possibilities for partitioning this solute. The solute could supersaturate the lattice, but this is energetically unfavorable especially in materials that have low lattice solubility, such as alumina. This process is also kinetically limited by relatively slow lattice diffusion. Excess solute could precipitate as second-phase particles. The activation energy of this process follows generally from heterogeneous nucleation theory. If strain effects are ignored this activation energy is generally

$$\Delta E = s\frac{\gamma_{\mathrm{int}}^3}{\Delta G_{\mathrm{f}}^2} \tag{1}$$

where γ_{int} is the interfacial energy, ΔG_{f} is the free energy of formation, and S is a proportionality constant that for isotropic systems is a geometric factor dependent on dihedral angle, but for anisotropic systems is more complex to derive. Another important option is for a complexion transition to occur. The more disordered complexions often display wider grain boundary regions and can accommodate more solute. As discussed above, it is known that the activation energy for the first transition is "relatively large", in that it is larger than the thermal energy available at temperatures near the onset of the first complexion transition. This transition can also lead to a reduction in grain boundary energy on the order of ~20–40%, but not every interface behaves the same. Between these processes, the most energetically favorable will dominate [36]. The process which occurs preferentially will produce a reduction in energy and will have a low activation energy. If the concentration of solute exceeds the solubility limit, then equilibrium predicts that precipitation should lead to a reduction in energy, but there is an associated activation barrier. Therefore, both precipitation and complexion transitions may reduce the total energy of the system, and both have activation barriers. Supersaturating the lattice will not reduce the energy of the system at any point, but may occur if the relative activation barriers to other transitions are sufficiently large. It is expected that in systems with low solubility and high-energy defects, like many ceramics, supersaturation is not a viable option to partition excess solute in a manner that minimizes free energy. For the current study of alumina, it is assumed that only complexion transitions and precipitation compete for partitioning excess solute.

Between complexion transitions and precipitation reactions, the process with the lower activation barrier will dominate. This is based on the fact that both processes reduce the energy of the boundary, and a previous observation that the limiting effect for the first complexion transition is the associated activation barrier [36]. Each process will occur with some finite probability, described by Boltzmann statistics. Based on this hypothesis, it is predicted from Eq. (1) that precipitates with low-energy interphase boundaries will have low activation barriers and will occur more frequently. The converse will also be true. Free energy of formation data is available from the literature [38–42]. Therefore, quantifying the relative energies of the interfaces between the lattice and the precipitate may provide insight into the relative activation energies of different precipitation reactions. If a relationship exists between the magnitude of the activation barrier and the propensity for complexion transitions, then new insight will be gained into the potential role of non-equilibrium thermodynamics in the stability of complexions and precipitates. In a sense, complexions may compete as an alternative "phase" in a phase selection process that occurs during microstructural evolution. The insight gained may lead to new additive selection criteria for controlling complexion behavior.

The surface dihedral angles of equilibrium thermal grooves have been used to measure the relative grain boundary to surface energy ($\gamma_{\mathrm{Gb}}/\gamma_{\mathrm{S}}$). The geometry of these grooves may be investigated using an analysis described by Mullins [43]. This analysis assumes isotropic surface energies and known grain boundary plane inclinations. However, it has been shown that by measuring a distribution of dihedral angles it is possible to average over these effects and obtain a meaningful average value [44]. Mullins [43] actually derived this analysis for half grooves, where the dihedral half-angle is used to determine the relative boundary to surface energy. The interphase boundary and grain boundaries share common surface distributions. This allows the relative energies of both boundary distributions to be quantified relative to the same surface distribution, and therefore one another.

The purpose of this paper is to test the hypothesis that doped aluminas that produce precipitates with low interphase energies are less likely to undergo complexion transitions than those that produce precipitates with high interphase energies. This will be done by measuring the relative energies of interphase boundaries between doped aluminas and their equilibrium precipitates. These data, combined with known free energies of formation, allow

relative activation barriers to be determined and compared to the existence of complexion transitions. Ca, Mg, Si, and Y were selected as dopants because their complexion transitions are known, and some of these additives promote abnormal grain growth while others suppress it.

2. Experimental procedure

Samples were fabricated by either hot-pressing undoped alumina powder around a bulk second-phase material, or by hot-pressing powder having the composition of the equilibrium second phase around undoped alumina.

Undoped alumina (Sumitomo AKP-HP, Sumitomo Chemical, Tokyo, Japan) was hot-pressed in a graphite die in vacuum at 1350 °C for 2 h at 40 MPa. Powder with a nominal composition of calcium hexaluminate (CA6) was prepared by mixing undoped alumina with calcium nitrate tetrahydrate (99.995%, Alfa Aesar) in ethanol. The mixture was ball-milled with alumina milling balls (99%) for 24 h, dried in a drying oven, and subsequently calcined at 800 °C for 2 h. Powder with nominal composition of magnesium aluminate spinel (spinel) was produced by mixing alumina powder with magnesium carbonate tetrahydrate in ethanol. This powder was also ball-milled, dried, and calcined in the same manner as the calcium hexaluminate. The dense undoped alumina sample was cut into pieces approximately 1 mm thick and 1 cm in diameter, and was polished to a 1 μm diamond finish. These pieces were placed into the calcium hexaluminate powder and spinel powder, separately. Pieces of c-plane, r-plane, and a-plane sapphire were also placed in the CA6 powder. These two sets of powders were both hot-pressed, separately, in graphite dies for 2 h at 1200 °C and 40 MPa. Because the CA6 and spinel form by reactive sintering around the undoped alumina, it is likely that some reaction between the dense alumina and the powder will occur. This may lead to some preferential crystallographic relationships between individual grains.

Dense lumps of crystalline silica of diameter ~1–3 mm were obtained from a commercial source (Alfa Aesar). Dense yttrium aluminum garnet (YAG) was also obtained from a commercial source (Baikowski, Japan). The YAG was polished to a 1 μm diamond finish and a piece approximately 1 mm thick and 1 cm in diameter was placed in undoped alumina. The silica was also placed, as-received, in undoped alumina. These two powders were hot-pressed, separately, in graphite dies at 1200 °C for 2 h under 40 MPa of pressure. The samples containing silica cracked during hot-pressing. This most likely occurred during cooling as a result of the phase change that occurs in silica. X-ray diffraction indicated that alumina was still present and that mullite had not formed. The silica samples were difficult to prepare because of a phase transition that occurs when cooling from high temperature. Small pieces of sample that were not cracked and broken were examined. The nature of these samples made them somewhat difficult to image, by atomic force microscopy (AFM), with low vibrational stability. There were few crack-free silica grain boundaries in the sample, so these grain boundaries were not measured.

Samples were cut such that the interphase boundary was approximately perpendicular to the sample surface. These samples were polished to a 1 μm diamond finish. Polishing was performed using diamond lapping films to minimize differential wear near the interface that may result from the differences in hardness. The CA6-, spinel-, YAG-, and silica-containing samples were thermally etched at 1300 °C for 1–12 h, due to varying etching rates of the different materials. The samples were thermally etched at the lowest temperature appropriate to form sufficient thermal grooves. No enhanced grain growth was observed near the interface, suggesting that complexion transitions were unlikely to have occurred here. Interfacial energy is a function of temperature, so not measuring the energies at temperatures closer to the relevant complexion transitions could affect the trends in the results. However, interfacial energy tends to decrease with increasing temperature and the systems that do not undergo complexion transitions until higher temperatures may be expected to have lower energies than those that undergo the transitions at lower temperatures. Therefore, measuring all of the samples at lower temperatures should tend to underestimate the expected trends in the data rather than enhance them. However, previous measurements of undoped alumina grain boundaries at 1400 °C and 2020 °C did not observe a change in the average relative energy (~3%) outside of experimental error. The result suggests that the boundary energies in alumina may not be a strong function of temperature outside of any complexion transitions that may occur.

The profiles of thermal grooves were measured using an AFM (Veeco di CP-II). Fig. 2 shows a schematic of a thermal groove at the interphase interface, and the relevant measured parameters. The thermal groove geometry may be used to extract the dihedral half-angle (Ψ_S) using the analysis developed by Mullins [43]. The dihedral half-angle of an isotropic material is related to the ratio of the grain boundary energy (γ_{Gb}) to surface energy (γ_S) through the following equation:

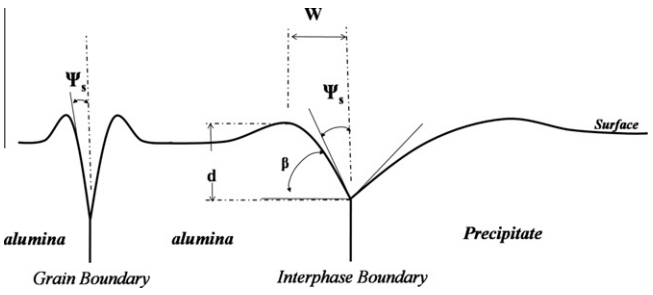

Fig. 2. Schematic of the cross-sectional view of a thermal groove formed where the surface intersects (left) a grain boundary and (right) an interphase boundary. The variables W and d are measured from groove profiles characterized by AFM, and Ψ is calculated.

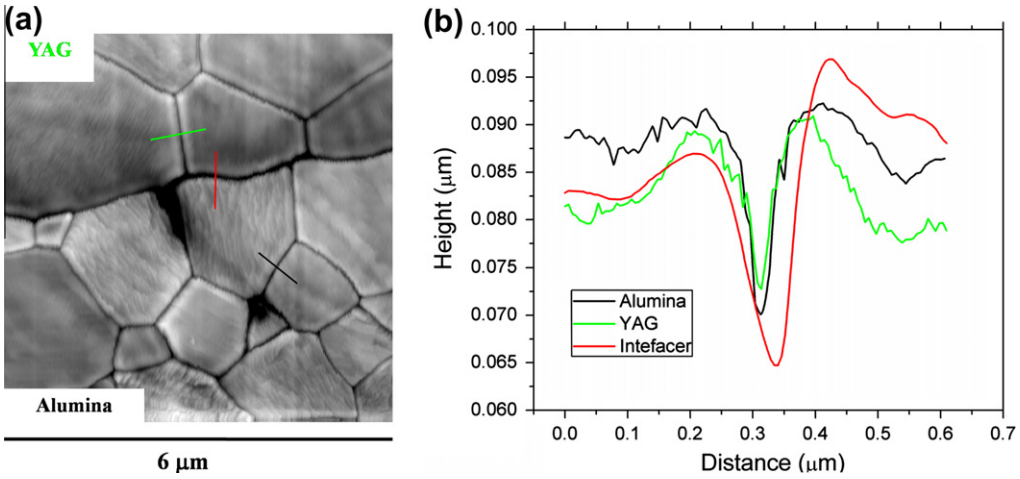

Fig. 3. (a) An AFM image of a YAG–alumina interface with lines indicating where the groove profiles shown in (b) were sampled.

$$\frac{\gamma_{Gb}}{\gamma_S} = 2\cos(\Psi_S) \quad (2)$$

Three measurements were made of each thermal groove. These measurements were used to calculate an average dihedral half-angle and a standard deviation. A scan resolution between 2 and 10 nm per pixel was used for all of the experiments. The effects of surface and interface anisotropy are dealt with by averaging a large number of measurements. An example of an interphase boundary and the corresponding thermal grooves are showing in Fig. 3. Average values of the relative energies provide a useful metric for comparing the different boundary populations. The sets of interfaces will share common surface distributions so the main variable will be the difference in average boundary energy. This means that γ_{Gb}/γ_S and γ_{int}/γ_S will be measured directly and the ratio of the two (γ_{int}/γ_{Gb}) will represent the relative fractional energy of the two interfaces. This measure is convenient because it is directly proportional to the actual interfacial energy, and given average grain boundary energy for alumina (for example 0.3 mJ m^{-2}) it would then be possible to directly calculate the interphase boundary energy.

The radius of curvature of the AFM tip may introduce artifacts into thermal groove geometry. Saylor et al. [44] detailed the effect of an AFM tip on this type of geometry and calculated the error as a function of the groove width and the surface inclination angle (β, which is the complementary angle to the thermal groove dihedral half-angle. For the YAG, spinel, and CA6 samples, this error was found to be less than the error experimentally determined by sampling each of the individual boundaries three times (~3°). The alumina–silica sample may likely have larger error, being underestimated by almost 10°, assuming a 60 nm tip radius. However, both the interphase boundary and the grain boundaries have been underestimated by approximately the same amount, which has little effect when comparing the relative energies of the two interfaces (the goal of the experiment).

3. Results

Representative images of the various interfaces are shown in Fig. 4. Some interfaces were faceted and some were rough. Most of the samples had slight differences in height due to differential polishing, although the differences were less than a few nanometers. The silica–alumina interface was difficult to characterize due to the cracking that had occurred during cooling. The cracking created rough exterior surfaces that made it difficult to mount the sample securely in the microscope and sample vibrations interfered with the imaging. The alumina grain size in these samples was quite small and some of the alumina grains seemed to have penetrated into the silica during hot-pressing, rather than forming a sharp interface. This is consistent with these samples having been hot-pressed at a low temperature where the first complexion transition was avoided and grain growth was minimal. The samples with silica and CA6 interfaces were annealed in a temperature range in which some grain boundary complexion transitions are observed in the bulk silica- and calcia-doped aluminas. However, no enhanced growth kinetics of the alumina were observed near the interphase boundary, suggesting that complexion transitions did not occur there. As discussed above, it may be necessary for grain boundaries to supersaturate prior to a complexion transition. Grain boundary supersaturation on either side of a diffusion couple (the interphase boundary here) will be difficult on short timescales. Supersaturation could occur in this case only if the boundaries first saturated and then grew sufficiently that the reduction in interfacial area produced significant supersaturation.

The surface dihedral half-angles on each side of each of these boundaries were measured separately and the results are shown in Figs. 5 and 6. They are reported as the angle of a certain phase either at the interface or at the grain boundary. This is describing which surface is being characterized at a particular interface. The surfaces are the

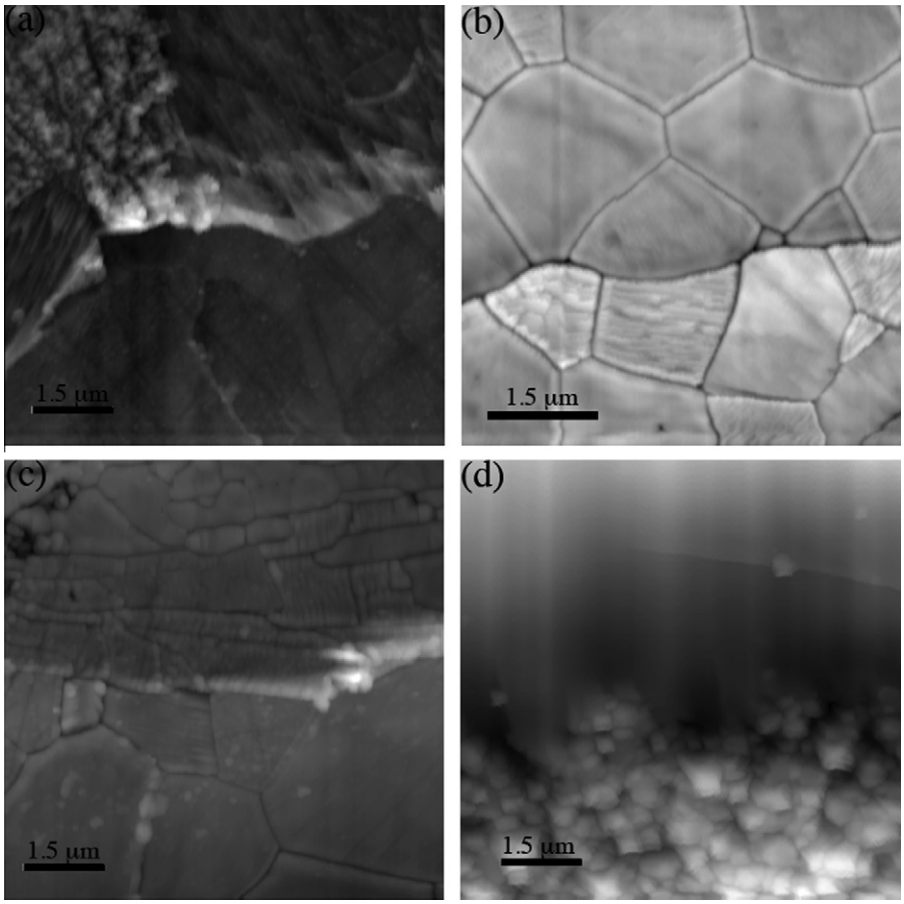

Fig. 4. Representative images of the interphase boundaries between alumina, which is at the bottom in each image, and (a) spinel, (b) YAG, (c) CA6, and (d) silica. The total scale height in each image is (a) 200 nm, (b) 75 nm, (c) 175 nm, and (d) 900 nm.

common feature that may be used to compare the relative grain boundary and interphase boundary energies. The results for the alumina–CA6 interface are not straightforward because the distribution of dihedral angles is bimodal (see Fig. 5c), whereas the other systems studied had single peaks in their distributions. The median dihedral angles for the interface between CA6 and A-, C-, and R-plane sapphire are also plotted in Fig. 5 as single points. The results suggest that the low-energy peak in the dihedral distribution is associated with the alumina basal planes and the higher energy peak is more closely associated with the A-planes. The morphology, flat platelets, also suggests that the low-energy peak in this distribution is related to the occurrence of interphase boundaries consisting of basal planes in the two systems. This result was confirmed by analysis of grooves at the interface between single crystal sapphire and polycrystalline CA6. This point will be detailed in the discussion. It should also be noted that large differences in dihedral angles were observed between the basal plane of plate-like CA6 grains and the ends of the same grain, when both interfaces were in contact with alumina. This result also confirms a significant anisotropy effect.

The results of the relative interphase to grain boundary energy ratio measurements are summarized in Table 1. Table 1 also contains information about the temperature range in which each material is likely to undergo a complexion transition. These temperatures are based on previous results [17]. It is hard to define an exact temperature, because the number of boundaries that undergo a transition increases exponentially with temperature [45], and these processes can be sensitive to background impurities. The change in free energy associated with the phase transformation is also a critical parameter in determining the activation energy. The free energies of formation for spinel, YAG, and CA6 from alumina and the other component oxides have been referenced from the literature [38–42], and will be used to approximate the free energy change associated with precipitation. The free energy of formation of silica in alumina is difficult to reference and it will be assumed that this may be comparable to that of mullite, which is the equilibrium second phase on the phase diagram. The free energies are considered at the temperature at which the first complexion transition occurs in each of the different cases. There is some discrepancy amongst sources for each of the systems and approximate values of 40 kJ mol^{-1}, 75 kJ mol^{-1}, 130 kJ mol^{-1}, 30 kJ mol^{-1}, and 90 kJ mol^{-1} have been chosen for spinel at 1650 °C, CA6 at 1550 °C, YAG at 1400 °C, silica at 1200 °C, and CA6 at 1200 °C, respectively. The ratio of the relative interfacial energy cubed to the change in free energy squared is

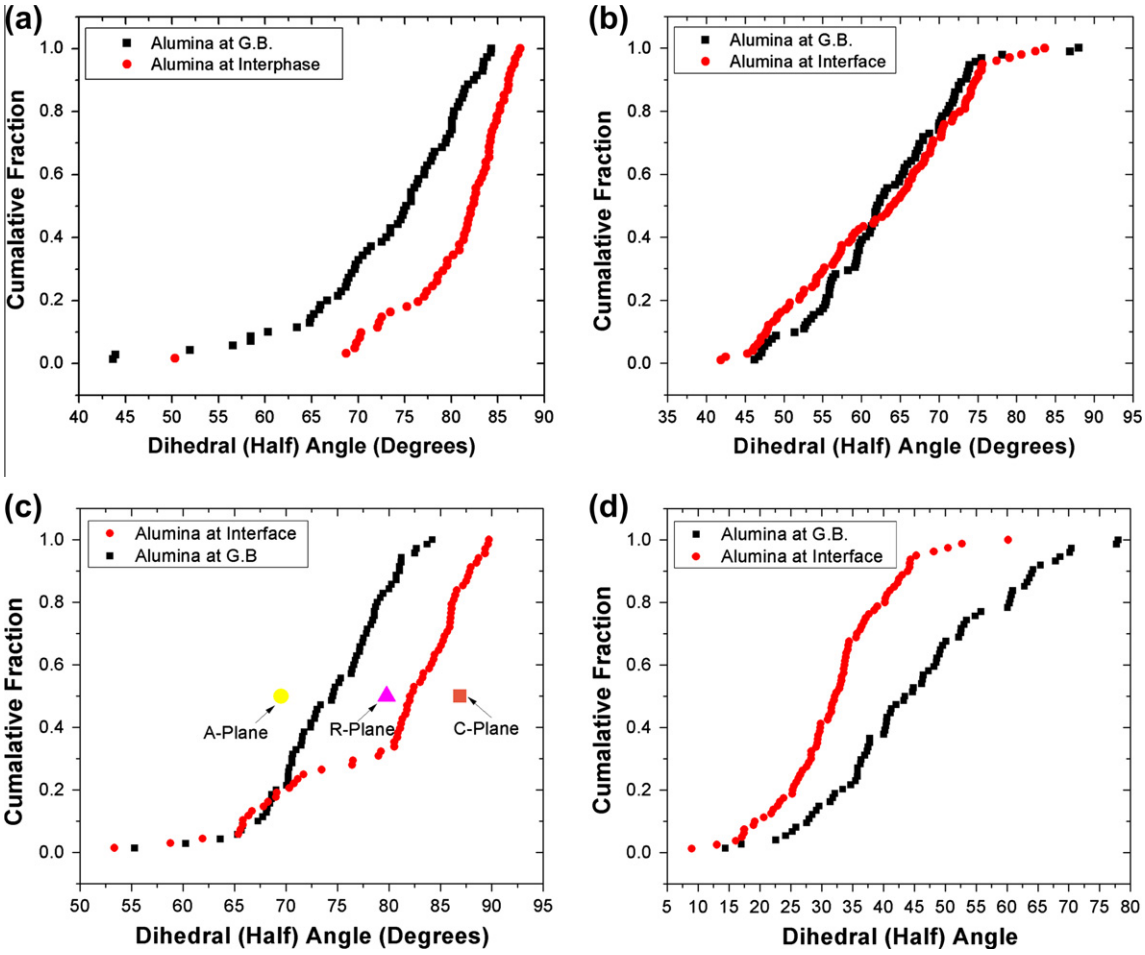

Fig. 5. Dihedral half-angles of the grain boundaries in the alumina samples and the dihedral half-angles on the alumina side of the interface with (a) spinel, (b) YAG, (c) CA6, and (d) silica. Also plotted in (c) is median dihedral half-angle occurring at the interface between CA6 and the A-, C-, and R-plane of alumina.

included in Table 1. This should represent the relative magnitude of the activation barriers to precipitation in each of the systems.

It is interesting to note that the interphase boundary energy is intermediate between the two sets of grain boundary energies (the alumina boundaries and the precipitate boundaries). Note that, in Figs. 5 and 6, silica grain boundaries were not measured as few crack-free silica grain boundaries existed in the samples. This suggests that, to some extent, the interphase boundary energy is an average of the two interfaces from which it is formed. This is similar to results that indicate that the energy of a grain boundary is proportional to the sum of the energies of the surfaces from which it comprises [46,47].

4. Discussion

4.1. General trends

There is a trend that dopants that form precipitates with lower interphase boundary energies tend to suppress complexion transitions relative to those with higher interphase boundary energies. This is quantified by the relationship between the interphase boundary energy and the temperature at which the first complexion transition is likely to occur. It is not likely that there is a direct relationship between these two quantities. Rather, precipitation and complexion transitions are competing effects and affecting the probability of one affecting the occurrence of the other. Theory predicts that the free energy of more disordered complexions is reduced with increasing temperature [17,18]. In most cases, precipitates will become less stable with increasing temperature (i.e. approaching the solidus). Both effects favor complexion transitions at higher temperatures, and precipitation at lower temperatures. The interfacial energy of the precipitate–matrix interface appears to influence where this crossover occurs for a particular interface. The behavior may also be closely related to the magnitude of the activation barrier. In the cases examined, the cubed surface term tends to dominate the squared volumetric term (see Table 1). The ordering of the relative activation barriers is not influenced by consideration of the free-energy term, except for the case of silica, where the results are the least reliable due to the free energy of formation being approximated from data for mullite.

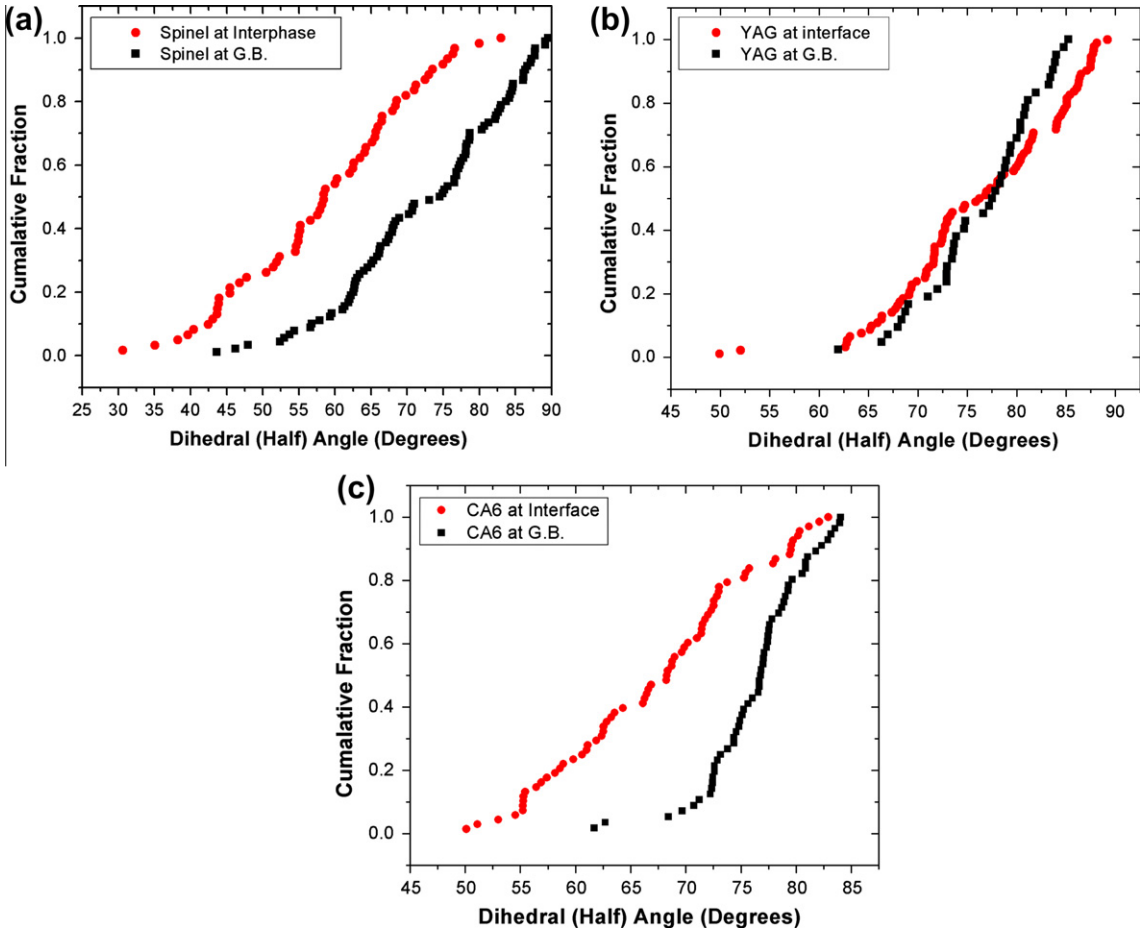

Fig. 6. Dihedral half-angles of the grain boundaries in the second phase and the dihedral half-angles on the (a) spinel, (b) YAG, (c) CA6, and (d) silica side of the interphase boundary.

Table 1
A list of the relative interphase boundary to alumina grain boundary energy ratio, the temperature at which the onset of abnormal grain growth begins in the associated system, the number of complexion transitions that system displays, and a factor representing the magnitude of the activation barrier that is the ratio of the relative interphase boundary energy cubed to the free energy of formation squared.

Phase (B)	$\gamma_{A/B}/\gamma_{Gb}$	Onset of 1st transition	Number of complexions	$(\gamma_{A/B}/\gamma_{Gb})^3/(DG_f)^2$ ($\times 10^5$)
Magnesium aluminate spinel	0.37	~1650–1750 °C	2	1.6
Calcium hexaluminate (basal)	0.51	~1550–1650 °C	3	2.4
YAG	0.9	~1400–1500 °C	5	4.3
Silica	1.13	~1200–1300 °C	5	90
Calcium hexaluminate (non-basal)	1.5	~1200–1300 °C	5	42

4.2. Local behavior and anisotropy

The results presented in Table 1 represent average quantities summed over many boundaries and surfaces. Complexion transitions and precipitation reactions are very local phenomena and will depend on local chemistry and anisotropy effects. In fact, multiple complexions and precipitates will coexist in a single microstructure. The discussion of the two processes competing in a material is not actually global, but is instead considered at individual grain boundaries. Understanding the distribution of both is likely to be the key to understanding the more general microstructural evolution. A major factor in affecting the local phenomena is grain boundary and interfacial energy anisotropy. This effect, in addition to anisotropic segregation effects, will play a role in affecting the anisotropy of complexion transitions. The results for the alumina–CA6 interface highlight the important role that anisotropy plays in this process. The basal plane of calcia-doped alumina is much less likely to undergo a complexion transition than other crystallographic planes in the same material, below the eutectic temperature [25]. It is found that the CA6 to basal plane alumina interface has a relatively low energy. It is known that CA6 and alumina show epitaxy on their

basal planes [48], which should produce a low-energy interface. This behavior causes complexion transitions to be suppressed on basal planes, even while they are occurring on other boundaries on the same grain. The effect leads to the plate-like morphology that often characterizes abnormal grain growth in alumina (see Fig. 1a). Anorthite, which precipitates when alumina is co-doped with calcia and silica, also has epitaxy on the basal plane and tends to produce abnormal grains with a plate-like morphology [49]. Complexion transitions on different interfaces may be quite complex, because basal planes in alumina are the least likely to undergo early complexion transitions, but seem to be most likely to show true grain boundary melting or complete wetting [50,51]. This effect may result from the fact that, since precipitation is favored at these interfaces, large amounts of second phase may accumulate there in the form of larger precipitates. There must be some threshold concentration necessary to produce complete wetting, and the basal planes may tend to be the first to reach this threshold during coarsening. The lower mobility of these interfaces also favors this situation, as particle–boundary detachment is less likely on these boundaries.

For each of the other systems, preferred orientation relationships have been demonstrated. The epitaxy between basal planes in CA6 and alumina has already been discussed. This tends to form a facetted boundary with a highly preferred interfacial plane [48]. In both spinel–alumina and YAG–alumina, preferred orientation relationships have been observed to form when materials are processed either from the melt or deposited as thin films [59–64]. In both cases, epitaxy can occur on different planes and the interfaces may be rough, suggesting less preference for a specific crystallographic plane. In the cristobalite–alumina system, as far as the authors are aware, epitaxy has been achievable only when the silica is doped and the silica is grown by thin film deposition methods (i.e. potentially far from equilibrium) [65]. The literature is somewhat consistent with the current results: CA6–alumina has a strongly preferred crystallographic plane, interfaces in the spinel–alumina and YAG–alumina systems are more isotropic and potentially low energy, and silica–alumina does not have a strongly preferred crystallographic plane and likely has high energy, as suggested by lack of epitaxy. It should be noted that all of these systems are expected to have energy anisotropy and that analysis of orientation relationships or morphology provides only a very qualitative sense of that anisotropy.

4.3. System-specific results

Details of the alumina–CA6 and alumina–silica systems have been discussed in detail above in relation to anisotropy effects. It has been generally known that silica and calica doping (and co-doping) promote abnormal grain growth and complexion transitions in alumina [34,52]. The relatively high activation energy for precipitation in silica-doped alumina and off-basal planes in calcia-doped alumina helps explain these results.

There has been some debate in the literature as to whether or not yttrium doping suppresses abnormal grain growth relative to a similarly processed undoped alumina [28,29,37,52,53]. It appears that if there is an effect it is not pronounced. This is consistent with the fact that the YAG–alumina interfacial energy is comparable to the alumina–alumina interfacial energy. This suggests that the role of yttria is relatively inert when it comes to affecting complexion transitions, unless it is part of a ternary system that might favor the precipitation of a phase other than YAG. Gulgun et al. [37] characterized the concentration of yttrium solute at alumina grain boundaries as a function of dopant concentration by analytical electron microscopy. They observed supersaturation of grain boundaries at certain levels of excess solute, beyond which the concentrations were reduced due to precipitation. One anomalous feature of these results is that the supersaturation occurs at concentrations in excess of those where some precipitation should occur. However, it is quite possible that the presence of some precipitates does not mean that the entire system is equilibrated. As discussed above, complexion transitions are very local events and these transitions will be concurrent with precipitation reactions. The quoted grain sizes and annealing conditions of the characterized grains, in the referenced study, would suggest that measurements had been performed on boundaries that had not undergone complexion transitions. The results indicate that grain boundary supersaturation is possible in this system and that there is an activation barrier associated with precipitation.

A previous study had recognized that the role of magnesia in preventing abnormal grain growth in alumina was its ability to prevent complexion transitions [17]. The current result explains the mechanism by which this occurs. The relatively low alumina–spinel interface energy curbs the tendency for complexion transitions. It is interesting to note that nickel oxide, which also precipitates a spinel phase, has been shown to produce a similar effect as magnesia in alumina [54,55]. Magnesia segregation is also known to make alumina behave more isotropically [10,11,13,15,56–58], which means that if complexion transitions do occur they are more likely to occur throughout the microstructure. This effect contributes to the ability of magnesia-doped alumina to maintain a relatively unimodal and equiaxed microstructure. Others have suggested that magnesia may act like a scavenger in alumina [56]. Magnesia is known to co-dissolve tetravalent cations in the alumina lattice, and might dissolve some level of divalent cations in the spinel phase that forms. These effects likely complement the fact that magnesia suppresses complexion transitions, when present at high enough concentrations, through the low energy of the alumina–spinel interface. Spinel precipitates may help to mitigate the effects of other additives or impurities in alumina by acting as lower energy nucleation sites for other second-phase particles that might precipitate.

4.4. New additive selection criterion

While the behavior of individual interfaces may be rather complex, the average trend is clear. Dopants in alumina that form equilibrium precipitates that have low host–precipitate interfacial energies tend to suppress complexion transitions. Precipitates with relatively large interphase boundary energies promote complexion transitions. This fundamental understanding provides a new criterion for dopant selection. Equilibrium phase diagrams may be used to predict which phase will precipitate. Predicting the interfacial energy is more difficult. Interfacial energies may be calculated from first principles, or measured experimentally. It has been suggested that surface energies are a good predictor of grain boundary and interfacial energies [46,68]. The current work shows that the average interphase boundary energy is intermediate between the average grain boundary energies of the two phases. Phases that have low surface and grain boundary energies should tend to form low-energy interphase interfaces. A list of phases ordered by their surface or grain boundary energies might be used in a simple manner for dopant selection. Note that this selection criterion has been somewhat simplified by ignoring the volumetric contribution to the activation energy of precipitation and anisotropy; however, it provides a reasonable starting point. The focus of this work has been the relationship between the onset of complexion transitions and the energetics of precipitation. It is expected that similar effects may also dominate at different types of phase boundaries, where a new phase must nucleate.

This new selection criterion may be utilized to control a number of transport processes such as grain growth, densification, creep, or oxidation. It may also provide new opportunities for engineering novel structures by controlling the distribution of second-phase particles and complexions. For example, single crystals of alumina have been grown from polycrystals that initially contain magnesium aluminate spinel particles [66,67]. By preferentially evaporating magnesia, and removing the spinel, it was possible to induce a complexion transition in a localized region, which resulted in the conversion of the polycrystal into a large single crystal.

The results are also of interest to the general phenomenon of abnormal grain growth in polycrystalline materials, both ceramic and metal. It has long been known that abnormal grain growth occurs at temperatures when precipitates become unstable [69–72]. The classic interpretation is that as the number of precipitates is reduced by dissolution, it is possible for critical de-pinning events to occur. Second-phase pinning reduces the driving force for grain growth, and the grain boundary velocity is affected locally by de-pinning events [73]. The current results suggest that as precipitates become thermodynamically unstable, a complexion transition may be energetically preferred. Complexion transitions influence the mobility of the grain boundaries rather than the driving force. Our previous results have shown that a sufficiently large amount of precipitates may pin grain boundaries even after complexion transitions have occurred [25]. However, the higher mobility grain boundary complexions will be more likely to de-pin from precipitates. Therefore, it is difficult to interpret whether particle–boundary de-pinning will result from the enhanced mobility that results from a complexion transition, a change in the density of precipitates, or both. The current results may explain why abnormal grain growth is often more robust than may be predicted from theories based solely on the effect of precipitates on the local driving force for grain growth [71]. An analysis of the mechanism for abnormal grain growth requires a thorough analysis of transport kinetics, characterization of the interface structure and chemistry, and investigation of the distribution of particles, pores, and solute.

4.5. Comparison to metallic systems

The current results also underscore a major difference between the evolution of doped ceramic and metallic systems. Many metallic systems are known to undergo a series of precipitate reactions. A classic example of this is the aluminum–copper system where Guinier–Preston zones, Θ, Θ', and Θ'' precipitates form as a function of time and temperature. These concurrent metastable transitions occur in order to minimize the activation barrier associated with forming the equilibrium phase. Most ceramic systems have much less freedom in the formation of intermediate phases due to the additional constraints imposed by Coulombic considerations in charge balance and defect formation. Therefore, some metallic systems may have a variety of options for partitioning solute that are not available to ceramic systems. However, it is interesting to note that it has still been difficult to elucidate the mechanism for abnormal grain growth in the aluminum–copper system [16].

Some complexion transitions are not observable by conventional lattice imaging in the transmission electron microscope, which makes them difficult to distinguish [17]. This difficulty is more pronounced in systems with short correlation lengths, such as metallic systems. Segregation-enhanced diffusion has been observed in a number of metallic systems, at the onset of abnormal grain growth [74,75]. Careful preparation and characterization has shown the existence of disordered complexions in metallic systems [16,76]. Similar behavior has been inferred or observed in other systems [74,75,77]. This fact, along with the current results, suggests that it might be useful to re-evaluate the mechanism for abnormal grain growth in a variety of systems. Understanding the correct mechanism for abnormal grain growth will provide new opportunities to control the phenomenon. The observed relationship between complexion transitions and precipitation in alumina suggests a new criterion for additive selection to control these transitions based on the interphase boundary energy and the activation energy of precipitation.

5. Conclusion

The relative energy of the interface between a precipitate and the host lattice affects the occurrence of complexion transitions. Chemistries that produce low-energy interphase interfaces tend to suppress complexion transitions, while those nucleating precipitates with high interfacial energies promote them. This explains the classically misunderstood phenomenon of the role of magnesia as a sintering aid in alumina. Magnesia doping produces spinel precipitates that have a low interfacial energy and prevent complexion transitions. Additives such as silica and calcia favor sub-eutectic grain boundary complexion transitions due to the relatively high energy interfacial energy of the precipitate. This may be explained in context of a phase selection competition in which the activation barrier to the complexion transition and precipitation compete with one another. The interphase boundary energies tend to be intermediate to the energies of the grain boundaries in the component systems. These facts lead to a novel additive selection criterion based on knowledge of interfacial energies.

Acknowledgements

The authors are thankful for the support of the National Science Foundation's Materials Research Science and Engineering Center program under Award Number DMR-0520425 and the Pennsylvania Department for Community and Economic Development.

References

[1] Coble RL. Patent 3 026 210; 1962.
[2] Bennison SJ, Harmer MP. Ceram Trans 1990;7.
[3] Monahan RD, Halloran JW. J Am Ceram Soc 1979;62.
[4] Harmer MP, Brook RJ. J Mater Sci 1980;15.
[5] Bennison SJ, Harmer MP. J Am Ceram Soc 1983;66.
[6] Baik S. J Am Ceram Soc 1986;69:C101.
[7] Berry KA, Harmer MP. J Am Ceram Soc 1986;69.
[8] Bateman CA, Bennison SJ, Harmer MP. J Am Ceram Soc 1989;72:1241.
[9] Bennison SJ, Harmer MP. J Am Ceram Soc 1990;73.
[10] Handwerker CA, Dynys JM, Cannon RM, Coble RL. J Am Ceram Soc 1990;73.
[11] Baik S, Moon JH. J Am Ceram Soc 1991;74:819.
[12] Bae SI, Baik S. J Am Ceram Soc 1994;77:2499.
[13] Soni KK, Thompson AM, Harmer MP, Williams DB, Chabala JM, Levi-Setti R. Appl Phys Lett 1995;66.
[14] Gavrilov KL, Bennison SJ, Mikeska KR, Levi-Setti R. J Mater Sci 2003;38:3965.
[15] Kim B-K, Hong S-H, Lee S-H, Kim D-Y, Hwang NM. J Am Ceram Soc 2003;86.
[16] Dennis J, Bate PS, Humphreys FJ. Acta Mater 2009;57.
[17] Dillon SJ, Tang M, Carter WC, Harmer MP. Acta Mater 2007;55:6208.
[18] Tang M, Carter WC, Cannon RM. Phys Rev Lett 2006;97.
[19] Bishop CM, Tang M, Cannon RM, Carter WC. Mater Sci Eng, A 2006;A422:1–2.
[20] Harmer MP. J Am Ceram Soc 2010;93.
[21] Dillon S, Harmer M, Luo J. JOM 2009;61:1–2.
[22] Luo J. Curr Opin Solid State Mater Sci 2009;12.
[23] Luo J, Chiang Y-M. Annu Rev Mater Res 2008;38.
[24] Luo J, Dillon SJ, Harmer MP. Microsc Today 2009;17.
[25] Dillon SJ, Harmer MP. J Am Ceram Soc 2007;91:2304.
[26] Dillon SJ, Harmer MP. J Am Ceram Soc 2008;91.
[27] Dillon SJ, Harmer MP. Acta Mater 2007;55:5247.
[28] MacLaren I, Cannon RM, Gülgün MA, Voytovych R, Popescu-Pogrion N, Scheu C, et al. J Am Ceram Soc 2003;86:659.
[29] Wang CM, Cargill GS, Chan HM, Harmer MP. Acta Mater 2000;48.
[30] Altay A, Gülgün MA. J Am Ceram Soc 2003;86.
[31] Cook RF, Schrott AG. J Am Ceram Soc 1988;71:50.
[32] Altay A, Gülgün MA. Key Eng Mater 2004:264–8.
[33] Kaplan WD, Muellejans H, Ruehle M, Roedel J, Claussen N. J Am Ceram Soc 1995;78.
[34] Brydson RR, Chen S-C, Riley FL, Pan SM-X, Rühle M. J Am Ceram Soc 1998;81:369.
[35] Ritchie RO, Zhang XF, de Jonghe LC. Mater Res Soc Symp Proc 2004;819.
[36] Dillon SJ, Rohrer GS, Harmer MP. J Am Ceram Soc 2010;93:1796.
[37] Guelguen MA, Voytovych R, Maclaren I, Ruehle M, Cannon RM. Interface Sci 2002;10:99.
[38] Rog G, Kozlowska-Rog A, Zakula-Sokol K. J Chem Thermodyn 1993;25.
[39] Waldbaum DR. Am Mineral 1965;50.
[40] Jacob KT, Jayadevan KP, Wasedam Y. J Am Ceram Soc 1998;81.
[41] Xu X, Wang C, Tu G. J Less-Common Met 1989;155.
[42] Mao H, Selleby M, Fabrichnaya O. CALPHAD: Comput Coupling Phase Diagrams Thermochem 2008;32.
[43] Mullins WW. J Appl Phys 1957;28.
[44] Saylor DM, Rohrer GS. J Am Ceram Soc 1999;82.
[45] Dillon SJ, Harmer MP. J Eur Ceram Soc 2008;28.
[46] Saylor DM, Morawiec A, Rohrer GS. J Am Ceram Soc 2002;85.
[47] Saylor DM, El Dasher B, Sano T, Rohrer GS. J Am Ceram Soc 2004;87.
[48] Mallamaci MP, Sartain KB, Carter CB. Philos Mag A 1998:77.
[49] Mallamaci MP, Carter CB. J Am Ceram Soc 1999;82.
[50] Kebbede A, Messing GL, Carim AH. J Am Ceram Soc 1997;80:2814.
[51] Powell-Dogan CA, Heuer AH. J Am Ceram Soc 1990;73.
[52] Voytovych R, Maclaren I, Gulgun MA, Cannon RM, Ruhle M. Acta Mater 2002;50:3453.
[53] Wang CM, Cargill III GS, Chan HM, Harmer MP, Williams DB. Inst Phys Conf Ser 2000;165.
[54] Jorgensen PJ, Westbrook JH. J Am Ceram Soc 1964:47.
[55] Cahoon HP, Christensen CJ. J Am Ceram Soc 1956:39.
[56] Gavrilov KL, Bennison SJ, Mikeska KR, Chabala JM, Levi-Setti R. J Am Ceram Soc 1999;82:1001.
[57] Park CW, Yoon DY. J Am Ceram Soc 2002;85:1585.
[58] Mukhopadhyay SM, Jardine AP, Blakley JM, Baik S. J Am Ceram Soc 1988;71:358.
[59] Krell A, Klimke J, Hutzler T. J Eur Ceram Soc 2009;29.
[60] Liu C-M, Chen J-C, Chen C-J. J Cryst Growth 2005;285.
[61] Liu C-M, Chen J-C, Chen C-J. J Cryst Growth 2006;292.
[62] Sieber H, Hesse D, Pan X, Senz S, Heydenreich J. Z Anorg Allg Chem 1996;622.
[63] Grabmaier JG, Grabmaier BC, Kersten RT, Plattner RD, Zeidler GJ. Phys Lett A 1973;43.
[64] Hay RS. Mater Res Soc Symp Proc 1990;183.
[65] Jewhurst SA, Andeen D, Lange FF. J Cryst Growth 2005:280.
[66] Dillon SJ, Harmer MP. J Am Ceram Soc 2007;90.
[67] Scott C, Kaliszewski M, Greskovich C, Levinson L. J Am Ceram Soc 2002;85:1275.
[68] Wolf D. J Mater Res 1990;5.
[69] Gladman T. Proc R Soc Lond A 1966:294.
[70] Gangulee A, D'Heurle FM. Thin Solid Films 1972;12.
[71] Suwa Y, Saito Y, Onodera H. Acta Mater 2007;55.
[72] Andersen I, Grong Ø, Ryum N. Acta Metall Mater 1995;43.
[73] Smith CS, Zener C. Trans AIME 1948;175.

[74] Divinski SV, Lohmann M, Herzig C, Straumal B, Baretzky B, Gust W. Phys Rev B 2005;71:104104-1.
[75] Molodov DA, Czubayko U, Gottstein G, Shvindlerman LS, Straumal BB, Gust W. Philos Mag Lett 1995;72:361.
[76] Luo J, Gupta VK, Yoon DH, Meyer III HM. Appl Phys Lett 2005;87.
[77] Schoumllhammer J, Baretzky B, Gust W, Mittemeijer E, Straumal B. Interface Sci 2001;9.